

Elastic anomaly for SrTiO₃ thin films grown on Si(001)F. S. Aguirre-Tostado,¹ A. Herrera-Gómez,¹ J. C. Woicik,² R. Droopad,³ Z. Yu,³ D. G. Schlom,⁴ P. Zschack,⁵ E. Karapetrova,⁵ P. Pianetta,⁶ and C. S. Hellberg⁷¹CINVESTAV-Queretaro, Libramiento Norponiente 2000, Real de Juriquilla Queretaro 76230, Mexico²Ceramics Division, National Institute of Standards and Technology, Gaithersburg, Maryland 20899, USA³Microelectronics and Physical Sciences Labs, Motorola Labs, 2100E Elliot Road, Tempe, Arizona 85284, USA⁴Materials Science and Engineering, Pennsylvania State University, University Park, Pennsylvania 16802, USA⁵University of Illinois, APS-UNICAT, Argonne National Lab, Argonne, Illinois 60439, USA⁶Stanford Synchrotron Radiation Laboratory, Stanford, California 94309, USA⁷Center for Computational Materials Science, Naval Research Laboratory, Washington, D.C. 20375, USA

(Received 3 March 2004; published 5 November 2004)

X-ray diffraction measurements have revealed a negative Poisson's ratio for SrTiO₃ thin films grown on Si(001). X-ray absorption fine-structure measurements demonstrate that this elastic anomaly is driven by the interfacial polarization of the SrTiO₃ layers. First-principles density-functional calculations support these conclusions. It is suggested that this phenomenon may be common for heteroepitaxial growth of materials that possess an ionic polarizability.

DOI: 10.1103/PhysRevB.70.201403

PACS number(s): 68.35.Gy, 68.37.Yz, 68.60.Bs

When a thin film is grown on a substrate that has a different lattice constant, the lattice constant of the film perpendicular to the film/substrate interface responds to the strain imposed on its lattice constant in the in-plane direction. For a thin cubic film grown on the (001) face of a thick cubic crystal, Poisson's ratio¹ describing the tetragonal distortion of the film due to the presence of the two, equivalent, in-plane strains is given by:²

$$\varepsilon_{\perp} = -2[\sigma/(1 - \sigma)]\varepsilon_{\parallel}. \quad (1)$$

As Poisson's ratio is typically greater than zero (it must lie between $-1 < \sigma < 1/2$) (Ref. 3), a film that is under compression in plane should expand out of plane and vice versa.

Recently, the driving force of the semiconductor industry to integrate transition-metal oxides with Si has led to the development of SrTiO₃ (STO) thin-film growth on Si(001) (Refs. 4 and 5). These films have served as the gate-oxide layer for metal-oxide field-effect transistors and as the buffer layer for III-V on Si semiconductor technology. In addition, ferroelectric thin films show promise for providing the confining potential to create quantum dots in Si for quantum computing.⁶ As STO is representative of a large class of oxides with the perovskite structure, it is imperative to understand the fundamental aspects of its thin-film epitaxy and, in particular, any anomalous behavior it may exhibit.

STO films with thicknesses of 40, 60, 80, and 200 Å were grown on Si(001) substrates using molecular-beam epitaxy. Details of the sample preparation are given in Ref. 5. In order to characterize the strain state of the STO films, high-resolution x-ray diffraction measurements, using a crystal analyzer, were performed at the STO(002), Si(004), STO(200), and Si(220) Bragg reflections.

Figure 1(a) shows the STO(002) x-ray diffraction data for the perpendicular lattice constant of the STO films. Clearly, the effect of the substrate is evident for samples thinner than ~80 Å. The STO(002) Bragg diffraction peak shifts to smaller values of 2θ , revealing an increase in the STO(002)

perpendicular lattice spacing for the thinner films.

Because the crystal structure of STO is simple cubic, whereas the crystal structure of Si is face-centered cubic, pseudomorphic growth of a thin STO layer on a Si(001) substrate results in a STO layer that is rotated around the Si[001] surface normal by 45°; i.e., STO[100]||Si[110]. The resulting in-plane lattice strain ε_{\parallel} of the STO layer is then determined by the Si(001) 1×1 surface unit-cell dimensions: $(a_{\text{Si}}/\sqrt{2} - a_{\text{STO}})/a_{\text{STO}} = -1.66\%$. ($a_{\text{Si}} = 5.431$ Å and a_{STO}

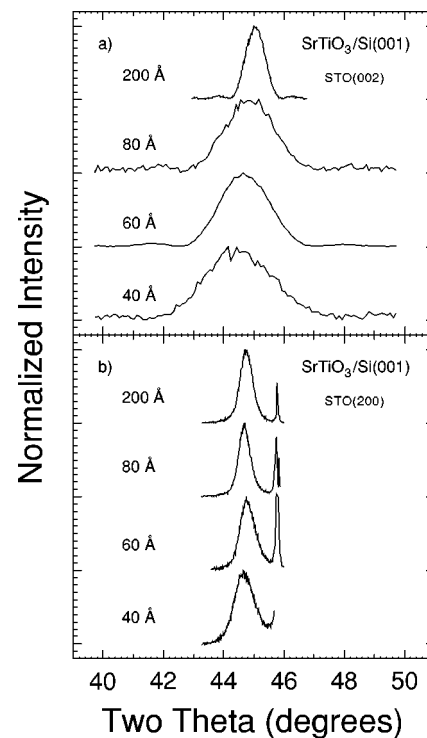


FIG. 1. (a) X-ray diffraction data around the STO(002) Bragg diffraction (out of plane). (b) X-ray diffraction data around the STO(200) Bragg diffraction (in plane).

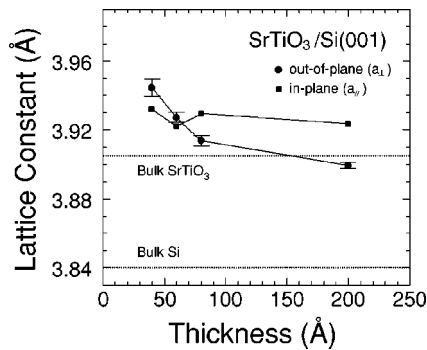


FIG. 2. In-plane and out of plane STO lattice constants for the 40, 60, 80, and 200 Å STO films. The dotted line shows the bulk cubic lattice constant of STO.

($a_{\perp}=3.905$ Å.) Using the macroscopic elastic constants of STO ($c_{11}=3.175 \times 10^{-12}$ dynes/cm² and $c_{12}=1.025 \times 10^{-12}$ dynes/cm²),⁷ this in-plane lattice strain translates to an out of plane lattice strain ϵ_{\perp} equal to +1.07%, which corresponds to a perpendicular STO lattice constant equal to 3.947 Å. From our STO(002) diffraction data, we determine the perpendicular lattice constant of the 40-Å film to be 3.945 ± 0.005 Å. These out-of-plane measurements by themselves would therefore suggest that the thinnest STO film becomes fully strained to match the in-plane Si lattice constant, and the tetragonal c/a distortion of the STO unit cell is $2.7 \pm 0.1\%$; i.e., $(c/a-1)=0.027$.

Figure 1(b) shows the glancing-incidence x-ray diffraction data recorded around the STO(200) in-plane Bragg diffraction condition. The sharp, intense peak occurring at larger 2θ is the in-plane Si(220) Bragg diffraction. Immediately evident from these data is that none of the STO layers are coherent with the Si(001) substrate as suggested by the out of plane STO(002) diffraction data. Had coherency between the STO and Si lattices been achieved, then the STO(200) and Si(220) Bragg diffractions would occur at the same $2-\theta$ value. The results of the diffraction experiment are summarized in Fig. 2. Most notably is the fact that the STO(200) lattice constant is significantly larger than the bulk STO lattice constant, opposite to what is expected for coherent, epitaxial growth on Si(001).

Rather, let us assume that the films relax to their bulk in-plane lattice constant at growth temperature (~ 700 °C). Because the thermal expansion coefficient of STO is larger than the thermal expansion coefficient of Si ($\alpha_{\text{STO}}=9 \times 10^{-6}$ K⁻¹ and $\alpha_{\text{Si}}=2.5 \times 10^{-6}$ K⁻¹),⁸ at room temperature the STO films will be under tensile, *not* compressive strain. Such thermal effects have been studied in detail for GaAs growth on Si(001).⁹ Using the thermal expansion coefficients of STO and Si, this growth mode produces an in-plane STO lattice constant equal to 3.923 Å at room temperature, which translates to an out of plane lattice constant equal to 3.894 Å, again using the macroscopic elastic constants of STO. Our experimental values for the in- and out of plane STO lattice constants for the 200-Å film are 3.923 ± 0.001 and 3.899 ± 0.002 Å, respectively. Therefore, it is clear that the thickest STO film relaxes on the Si substrate at growth temperature with its in- and out of plane lattice constants dic-

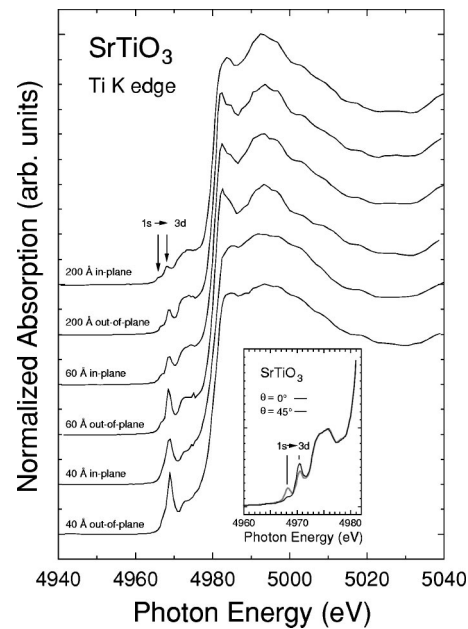


FIG. 3. Ti *K* near-edge x-ray absorption spectra from the thin STO films recorded with the polarization vector in plane and out of plane. The data have been normalized to equal edge jump. The energy positions of the $1s \rightarrow 3d$ transitions are indicated. The inset shows the pre-edge region of a bulk SrTiO₃ single crystal.

tated by the differential thermal contraction between STO and Si and the Poisson's ratio of bulk STO, which is positive.

The above analysis accounts for the tetragonal distortion observed in the 200-Å film, as well as for the in-plane lattice constants of the thinner films (that average to 3.927 Å). However, it in no way explains the increase in the out of plane lattice constant for the thinner films. In order to understand the microscopic distortions that lead to this phenomenon, we turn to our extended x-ray absorption fine-structure (EXAFS) data.

Near and extended x-ray absorption fine-structure data were collected at the Ti *K* edge ($h\nu=4966$ eV) by monitoring the Ti K_{α} -fluorescence emission using a single-element SiLi detector fixed in the horizontal plane at right angle to the incident photon beam. The absorption data were collected in two orientations, with the polarization vector ϵ of the synchrotron radiation aligned either parallel (ϵ in plane) or perpendicular (ϵ out of plane) to the Si(001) surface. Consequently, due to the two-dimensional nature of the surface/film/substrate geometry, it was possible to distinguish in-plane from out of plane Ti-O bonding. In addition, the x-ray absorption spectrum from finely ground STO powder was measured in transmission; it was used as the EXAFS phase and amplitude standard to *experimentally* determine the Ti-O bond lengths within the films.

Figure 3 shows the Ti *K* x-ray absorption near-edge spectra from the thin films studied. The spectra have been scaled to equal edge jump. The pre-edge features occur in the region of 4965–4980 eV. As is well known, in pure octahedral (O_h) symmetry the transition-metal $3d$ states are split by the ligand-crystal field into a triply degenerate t_{2g} set and a doubly degenerate e_g set, with a splitting of ~ 2 eV, as indicated

in Fig. 3. In molecular point groups that lack inversion symmetry, for example the tetrahedral (T_d) point group, the metal $4p$ orbitals mix with the metal $3d$ orbitals, but this mixing occurs only with the higher of the two crystal-field split metal $3d$ states.¹⁰ This $p-d$ mixing (or chemical hybridization on the metal site) makes $1s \rightarrow 3d$ transitions are dipole forbidden.¹¹ For this reason, the intensity of the second pre-edge feature is correlated with ferroelectricity in the perovskite structure;¹² i.e., with the quantitative displacement of the central Ti cation from its centrosymmetric position within the perovskite unit cell.

Our data show a large increase in intensity of the second but not the first Ti K pre-edge feature with decreasing STO film thickness. As a tetragonal c/a distortion of the Ti-O octahedra alone would not remove the center of inversion symmetry,¹⁰ these data indicate that the presence of the STO/Si interface results in the polarization of the STO layer. As evidenced by the data from the thicker films, this polarization decreases away from the interface, and it is likely caused by the ionic rearrangement of the first STO layer. Interfacial dipoles have been shown to influence the Schottky barrier height at metal-oxide/Si interfaces.¹³ They also exist at clean metal-oxide surfaces and are caused simply by a relaxation and “rumpling” of the surface layer normal to the surface.¹⁴

In order to quantify the extent of the observed polarization, the Ti-O radial shell was modeled with the EXAFS phase and amplitude functions obtained from the bulk STO powder. As anticipated, data recorded from the 200-Å film in either polarization were indistinguishable from bulk STO. The results of the modeling for the 60-Å film are shown in Fig. 4. (Results for the 40-Å film are similar, but with larger errors.) The top panel shows the fit to the data from the 60-Å film recorded with the polarization vector in plane, and the middle panel shows the fit to the data from the 60-Å film recorded with the polarization vector out of plane, both assuming a single Ti-O bond length. Clearly, a beat occurs in the out of plane data near $k=7 \text{ \AA}^{-1}$ that is not modeled by a single Ti-O distance. Our analysis therefore finds the Ti-O bond length to be split by $0.22 \pm 0.06 \text{ \AA}$ along the STO[001] surface normal direction.

To understand the significance of the volume increase observed in Fig. 2, first-principles density-functional theory (DFT) calculations were performed for STO supercells. The VASP plane-wave code¹⁵ was used, and the in-plane lattice constant of the supercells was constrained to be equal to the in-plane lattice constant of the STO films as determined by x-ray diffraction (3.927 \AA).¹⁶ Periodic supercells containing $\sqrt{2} \times \sqrt{2} \times N$ unit cells were used to accommodate the rotation of the oxygen octahedra. To mimic the polarization of the interface as determined by EXAFS, a single Ti-O layer was polarized in the normal direction by constraining its z coordinates to lie in planes 0.22 \AA apart. All other atomic coordinates were fully relaxed. The dependence of the calculated equilibrium lattice constant (calculated as the average of the individual layer spacings) as a function of numbers of layers N is shown in Fig. 5. Remarkably, it exhibits the same qualitative behavior as observed in Fig. 2.

We also considered the possibility of Si diffusion into the

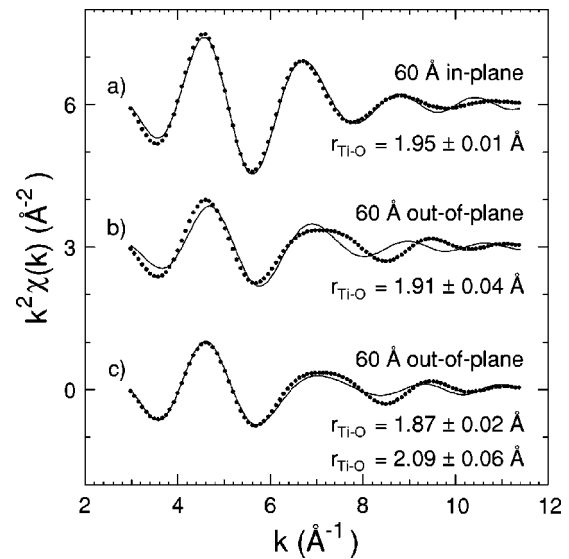


FIG. 4. Fits to the Fourier-filtered, first-shell contributions to the k^2 -weighted Ti K -edge EXAFS from the 60-Å film using the phase and amplitude functions obtained from the STO powder. The dots are the data points of the back transform, and the solid lines are the fits. (a) In-plane data using one Ti-O distance. (b) Out of plane data using one Ti-O distance. (c) Out of plane data using two Ti-O distances.

STO. Using DFT, we examined the energetics and volume changes resulting from Si atoms in $3 \times 3 \times 3$ supercells of bulk STO both with and without an oxygen vacancy. We find an energy cost of 4.6 eV for a Si interstitial in pure STO, and 3.9 eV to place a Si atom near an oxygen vacancy. In the former case, the supercell volume increased by 1.4%; in the latter, the increase is 1.0%. Thus, an unreasonably high density of Si interstitials are required to cause the observed expansion.

Let us now ponder the genealogy of this anomalous behavior. It is well known that a c/a distortion accompanies the ferroelectric phase transition in the cubic perovskites. This spontaneous polarization arises from a net displacement of the positive and negative ions within the unit cell together with the concomitant loss of inversion symmetry. For BaTiO₃, the c/a distortion of its tetragonal phase is $\sim 1\%$.¹⁷ This distortion compares with the value determined by x-ray

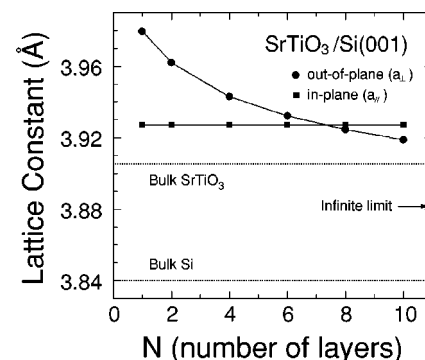


FIG. 5. Calculated out of plane STO lattice constants as a function of supercell size.

diffraction for the thinnest STO film, $\sim 0.33\%$. Consequently, the driving force of this anomaly is the polarization of the STO layer in the vicinity of the STO/Si interface. Apparently, it is energetically favorable for the out of plane lattice constant of a polarized film to be larger than its in-plane lattice constant ($c/a > 1$), even though the in-plane lattice constant is under tensile strain. As it is the macroscopic polarization and its intrinsic relationship to strain that results in the observed elastic anomaly, similar behavior may be common in the heteroepitaxial growth of materials that possess an ionic polarizability.

This research was carried out (in part) at the National Synchrotron Light Source, Brookhaven National Laboratory, which is supported by the U.S. Department of Energy (DOE), Division of Materials Sciences and Division of

Chemical Sciences, under Contract No. DE-AC02-98CH10886. The UNICAT facility at the Advanced Photon Source (APS) is supported by the University of Illinois at Urbana-Champaign, Materials Research Laboratory (U.S. DOE, the State of Illinois-IBHE-HECA, and the NSF), the Oak Ridge National Laboratory (U.S. DOE under contract with UT-Battelle LLC), the National Institute of Standards and Technology (U.S. Department of Commerce), and UOP LLC. The APS is supported by the U.S. DOE, Basic Energy Sciences, Office of Science under Contract No. W-31-109-ENG-38. Additional support was provided by the Consejo Nacional de Ciencia y Tecnología de México (CONACyT Project No. 34721-E, 33901-U), the Stanford Linear Accelerator Center (CRADA—Project No. 158), and by the DARPA QuIST program. Computations were performed at the ASC DoD Major Shared Resource Center.

-
- ¹L.D. Landau and E.M. Lifshitz, *Theory of Elasticity* (Pergamon, Oxford, 1970).
- ²J. Hornstra and W.J. Bartels, *J. Cryst. Growth* **44**, 513 (1978).
- ³N.R. Keskar and J.R. Chelikowsky, *Nature (London)* **358**, 222 (1992).
- ⁴R.A. McKee, F.J. Walker, and M.F. Chisholm, *Phys. Rev. Lett.* **81**, 3014 (1998).
- ⁵Z. Yu, J. Ramdani, J.A. Curless, J.M. Finder, C.D. Overgaard, R. Droopad, K.W. Eisenbeiser, J.A. Hallmark, and W.J. Ooms, *J. Vac. Sci. Technol. B* **18**, 1653 (2000).
- ⁶J. Levy, *Phys. Rev. A* **64**, 052306 (2001).
- ⁷R.O. Bell and G. Rupprecht, *Phys. Rev.* **129**, 90 (1963).
- ⁸D.R. Lide, *CRC Handbook of Chemistry and Physics*, 80th ed. (CRC, 2000), p. 1297.
- ⁹N. Lucas, H. Zabel, H. Morkoc, and H. Unlu, *Appl. Phys. Lett.* **52**, 2117 (1988).
- ¹⁰F.A. Cotton, *Chemical Applications of Group Theory* (Wiley, New York, 1971), Chap. 8.
- ¹¹J. Wong, F.W. Lytle, R.P. Messmer, and D.H. Maylotte, *Phys. Rev. B* **30**, 5596 (1984).
- ¹²B. Ravel, E.A. Stern, R.I. Vedrinskii, and V. Kraizman, *Ferroelectrics* **206–207**, 407 (1998).
- ¹³R.A. McKee, F.J. Walker, M.B. Nardelli, W.A. Shelton, and G.M. Stocks, *Science* **300**, 1726 (2003).
- ¹⁴A. Munkholm, S.K. Streiffer, M.V.R. Murty, J.A. Eastman, C. Thompson, O. Auciello, L. Thompson, J.F. Moore, and G.B. Stephenson, *Phys. Rev. Lett.* **88**, 016101 (2001).
- ¹⁵G. Kresse and J. Hafner, *Phys. Rev. B* **47**, R558 (1993); G. Kresse and J. Furthmuller, *ibid.* **54**, 11169 (1996); G. Kresse and D. Joubert, *ibid.* **59**, 1758 (1999).
- ¹⁶The generalized gradient functional was used, which typically overestimates lattice constants and gives 3.9445 Å as the bulk lattice constant of STO. Therefore, all lattice constants were rescaled by 3.9445/3.905 in the calculations. Projector augmented wave potentials and a plane-wave cut off of 400 eV were used. We used $4 \times 4 \times M$ Monkhorst-Pack sampling of the Brillouin zone, where $M \geq 6/N$ for a supercell with N layers.
- ¹⁷G.H. Kwei, A.C. Lawson, S.J.L. Billinge, and S.-W. Cheong, *J. Phys. Chem.* **97**, 2368 (1993).